

Protein aggregate formation permits millennium–old brain preservation

Axel Petzold ¹ Ching-Hua Lu ² Mike Groves ³
Johan Gobom ⁴ Henrik Zetterberg ⁵ Gerry Shaw ⁶
Sonia O'Connor ⁷

Manuscript version: 8-jan-2020

Correspondence UCL Institute of Neurology, Department of Molecular Neuroscience, Queen Square, London, WC1N 3BG, UK.

Email: a.petzold@ucl.ac.uk

¹Department of Neuroinflammation and National Hospital for Neurology and Neurosurgery, UCLH, Queen Square, WC1N 3BG; Moorfields Eye Hospital, City Road, EC1V 2PD, London, United Kingdom; Neuroscience Campus Amsterdam, Departments of Neurology and Ophthalmology, Amsterdam, NL

²Neurology, School of Medicine, China Medical University and Hospital, Taichung City, Taiwan & Sobell Department of Motor Neuroscience and Movement Disorders, UCL Institute of Neurology, Queen Square, London, UK

³Devison of Neuropathology, UCL Institute of Neurology, Queen Square, London, United Kingdom

⁴Department of Psychiatry and Neurochemistry, Institute of Neuroscience and Physiology, The Sahlgrenska Academy at the University of Gothenburg and Clinical Neurochemistry Laboratory, Sahlgrenska University Hospital, Mölndal, Sweden

⁵UK Dementia Research Institute at UCL, London WC1E 6BT, U.; Department of Neurodegenerative Disease, UCL Institute of Neurology, Queen Square, London WC1N 3BG, UK

⁶EnCor Biotechnology Inc., 4949 SW 41st Boulevard, Ste 40., Gainesville, FL 32608, USA

⁷Archaeological and Forensic Sciences, University of Bradford, Richmond Road, Bradford, West Yorkshire, BD7 1DP, UK

Abstract

Human proteins have not been reported to survive in free nature, at ambient temperature, for long. Particularly the human brain rapidly dissolves after death due to auto-proteolysis and putrefaction.

The here presented discovery of 2,600 year old brain proteins from a radiocarbon dated human brain provides new evidence for extraordinary long-term stability of non-amyloid protein aggregates.

Immuno electron microscopy confirmed preservation of neurocytoarchitecture in the ancient brain, which appeared shrunken and compact compared to a modern brain. Resolution of intermediate filaments (IFs) from protein aggregates took 2–12 months. Immunoassays on micro-dissected brain tissue homogenates revealed preservation of the known protein topography for grey and white matter for type III (glial fibrillary acidic protein, GFAP) and IV (neurofilaments, Nfs) IF. Mass spectrometry data could be matched to a number of peptide sequences, notably for GFAP and Nf. Preserved immunogenicity of the prehistoric human brain proteins was demonstrated by antibody generation (GFAP, Nf, myelin basic protein). Unlike brain proteins, DNA was of poor quality preventing reliable sequencing.

These long-term data from a unique ancient human brain demonstrates that aggregate formation permits for preservation of brain proteins for millennia.

Keywords Biomarker, neurofilament, glial fibrillary acidic protein, protein aggregation, neurodegeneration, archaeology.

Abbreviations: CNS = central nervous system, CTRL = control group, ELISA = enzyme linked immunoabsorbant assay, GFAP = glial fibrillary acidic protein, GM = gray matter, IF = intermediate filaments, MBP = myelin basic protein, MRI = magnetic resonance imaging, MW = molecular weight markers, Nf = neurofilaments, NfH = neurofilament heavy chain, NfL = neurofilament light chain, WM = white matter.

1 Introduction

Understanding mechanisms of preservation of proteins is relevant at the interface between biomedical applications [1], protein biomarker research [2] and medicine [3].

In free nature, protein preservation is a conundrum because spontaneous decomposition is a feature of all biological macromolecules caused by simple chemical processes [4, 5]. Therefore the yellowish brown mass seen through the foramen magnum of an Iron Age human skull (cranium OxA-20677 collagen radiocarbon dating 673-482 BC [6]) from archaeological excavations in Heslington, York, UK, offers a unique opportunity to use molecular tools [7] to investigate the preservation of human brain proteins.

The preservation of this human brain tissue remains a mystery in view of decomposition and autolysis starts within minutes after death [8, 9]. Compared to other body parts such as bones [10], autolysis is particularly rapid in the brain, which consists of 80 percent water [9, 11]. Biochemically, autolysis is caused by massive activation of proteases and phospholipases destroying the molecular structure of lipids and proteins [8, 12]. Within 36–72 hours, putrefaction starts and complete skeletonisation results within 5–10 years [12, 13]. In conclusion, preservation of human brain proteins at ambient temperature should not be possible for millennia in free nature [4, 5, 7, 8, 11–13]. For this reason taxonomic studies of the brain of human evolutionary descent relied until recently mainly on the discussion of skull fragments

and teeth [10, 11]. New data on stability and binding affinities of proteins have however advanced the development of evolutionary models [14]. These mainly sequence based data [14] are now also enriched by protein biophysics data [15]. The thermodynamic stability of a protein is related to its structure [16, 17]. It is more challenging to unfold a very stable protein compared to an unstable protein [15]. Protein stability provides indirect evidence for protein function and is driven by mutations influencing protein structure [14, 18].

The human brain is in particular need of structural stability because the key components, neurons and axons do not normally regenerate. The cellular scaffold of neurons and their supporting cells, astrocytes, consists of intermediate filaments (IF). These IF represent a group of protein polymers which are classified by fibre diameter (8-12 nm) as *intermediate* between the smaller microfilaments (7 nm) and the larger microtubules (≈ 25 nm) [19]. The IF of neurons/axons are neurofilaments (Nfs) [20, 21] and the IF of astrocytes are glial fibrillary acidic protein (GFAP) [22, 23]. This cellular specificity has been of advantage for the development of GFAP and Nf proteins as body fluid biomarkers for disease, amongst many other proteins [2, 21, 24, 25]. In addition, IF have a number of unusual protein features because they are intrinsically unstructured, have large polyanion tails, multiple phosphorylation sites, are able to self-assemble into polymers and form intra- and extracellular aggregates in pathology [26–33]. Particularly the ability to form protein aggregate is thought to be relevant for progression of neurodegeneration [26, 34].

Taken together the data presented in this study on protein stability from the unique find of a preserved prehistoric human brain [6] is of mutual benefit to the fields of protein biomarker research [2, 20, 24, 25, 35], medicine [3, 26, 34], structural and functional proteomics [14, 18], biomedical applications [1] and archaeology [6, 10, 11].

2 Results

The data of this translational study are presented by moving from Archaeology to biochemistry and from macro-structure over micro-structure to proteomics.

2.1 Preservation of the macro-structure of a 2,600 year old human brain

Mummification permits long term preservation of soft tissue. Natural mummification was responsible for the preservation of the brain of the iceman, who was preserved in a glacier [36]. In contrast to the iceman and most other previously reported finds of preserved human brains, there were no sign of hair, skin or any other soft tissue associated with the ancient brain subject to the present study (Figure 1 A) [6]. A yellowish brown mass (Figure 1 B) was seen through the foramen magnum of a human skull in Heslington, York, UK excavated by the York Archaeological Trust in August 2008. The identification of this putative brain tissue was strengthened following craniec-

tomy (Figure 1 C). Although covered by sediment (Figure 1 D), individual brain gyri became discernible after cleaning (Figure 1 E). Collagen from the bone was radiocarbon dated (OxA-20677) to 673-482 BC [6]. There was no evidence for tannins or artificial preservation techniques [6].

The preservation of the ancient brain tissue remains enigmatic because of rapid decomposition and autolysis after death [8, 9].

2.2 Ancient brain histology

Consistent with the macrostructure (Figure 1 E) the micro-structure of the ancient brain also resembled remnants of brain tissue axons (Figure 2 A). The electron microscopy (EM) images showed 5–10 μm long and 0.2–0.6 μm thick filamentous, electron-dense structures (Figure 2 A). In axial sections the diameter of these axonal structures ranged from 0.2–4 μm . These ancient axons were more densely packed than axons from a contemporary human brain sample (Figure 2 B). Contemporary axons were longer (up to 17.3 μm) and of larger diameter (0.8–7.5 μm). These data suggest diagenetic alterations.

Next, a monoclonal antibody was used to test the hypothesis that the exceptional preservation of axonal structures did contain highly specific axonal proteins. Neurofilament (Nf) proteins represent a family of differently sized isoforms expressed in neuronal tissue [19, 20]. Specific immuno-EM to the Nf heavy chain (NfH) showed strong binding to the filamentous structures present in the suspected shrunken axons (Figure 2 C). At higher magnifi-

cation, the gold-labelled anti-NfH antibodies lined up exclusively alongside the compact filamentous structures elongated inside the axons (Figure 2 D). The exclusive binding of the gold particles to the axonal structures confirms the morphological EM observations.

Further verification that the preserved filamentous axonal structures contain ancient, but intact protein epitopes can be obtained by reversal of the experimental setup. No detailed studies have yet been conducted on the suspected preservation of immunogenic ancient protein epitopes. We therefore proceeded with generation of polyclonal antiserum against the Heslington brain.

2.3 Antibody generation

In order to screen for potential preservation of antigenic epitopes from other human brain proteins, antibodies against the ancient brain were generated in mice. Both white (WM) and gray matter (GM) of the ancient brain tissue produced a robust immune-response (titres 1:2,000) to glial fibrillary acidic protein (GFAP) and myelin basic protein (MBP) as shown by staining against E21 rat cortical neuron cultures (Figure 2 E–J). Elements of the mouse serum staining pattern clearly resembled oligodendrocyte (Figure 2 E) and astrocytic cells (Figure 2 H). Double label with antibodies to MBP (Figure 2 F) showed exact overlap in cells with an oligodendrocyte morphology, while cells with an astrocytic morphology (Figure 2 H) showed perfect overlap with GFAP antibody (Figure 2 I, J). Western blotting on pure MBP

and pure GFAP showed that mouse serum stained pure MBP (Figure 2 K, lane 1) as well as a bone fide MBP antibody (lane 2), and that it stained pure GFAP (lane 3) as well as a bone fide GFAP antibody (lane 4). For Nf a weaker immune–response was found which did not mature and bands were less distinct on the immunoblot. There was no hint of this pattern of staining from the mice blood samples taken prior to injection (1:100). In conclusion, these experiments demonstrated strong immunogenicity for ancient GFAP and MBP, and to a lesser extend for Nf.

2.4 Ancient brain homogenate contains high molecular weight protein aggregates

To further investigate these protein candidates, GM and WM samples were taken from the ancient and a modern human control brain. The median wet weight of the ancient brain samples (0.076 g, n=10) was comparable to the control tissue samples (0.104 g, n=10, p=0.13). Samples were homogenised, centrifuged and the supernatant taken for analysis of the soluble protein fraction. Much of the ancient brain material remained insoluble being visible as small brown particles. The total protein concentration of the ancient brain was significantly lower (median 0.359 g/L) compared to control brain tissue (1.302 g/L, p<0.01). There was a good correlation of the wet weight with the total protein concentration (R=0.72, p=0.018, Figure 3 A) indicating that the proportion of soluble protein from all samples was comparable despite the

remaining insoluble fraction. Gel-electrophoresis of the ancient brain showed multiple agrophil bands (Figure 3 B). The band pattern was consistent between samples and increased in density with higher protein load. Immunoblotting showed faint binding for hyperphosphorylated Nf (NfH^{SMI34}) in the higher molecular range (420 kDa, Figure 3 C). This was about two times the expected gel migration around 220 kDa [20, 31, 33, 37]. It seemed therefore likely that protein aggregate formation had occurred [38]. The aggregates from the ancient brain were larger and considerably more resistant to incubation with urea as those from recent human or animal brains [15, 20, 31, 37–40].

2.5 IF iso- and phosphoforms discriminate brain structures and show a pattern reversal between ancient and modern control tissue

Taken together, the qualitative histological and immunological data suggested presence of quantifiable amounts of soluble Nf, GFAP and MBP in the ancient brain. We hypothesised that if preservation occurred quickly enough it should still be possible to discern GM from WM samples. These proteins are present in a higher concentration in the WM compared to the GM [39, 41, 42]. Surprisingly, the GM and WM protein concentrations from the ancient brain were inverse to the control brain (Figure 3 D–H) and the data from the literature [39, 41, 42]. Consistent with the well known higher susceptibility

of non-phosphorylated NfH to proteases compared to phosphorylated NfH [43, 44], absolute levels of the non-phosphorylated NfH^{SMI38} were lower in the control brain compared to the phosphorylated NfH^{SMI34} and NfH^{SMI35}. Additionally, the Nf light chain which is known to be less stable than the phosphorylated heavy chain [43–45] was present at a higher absolute concentrations in the ancient brain than NfH (Figure 3 G). Combined, the data suggest that the proteases of the ancient brain might have been inhibited by an unknown compound which had diffused from the outside of the brain to the deeper structures.

Chemically, preservation might have been possible by an acidic compound similar to what is known from soft tissue preservation of the Bog bodies with a pH about 3.5 from the beautifully preserved Danish examples [46]. The tissue pH of the ancient brain was 4.6, but we would be hesitant to use this as a proxy for the burial environment. The pH of a burial environment can vary spatially over very small distances and changes with time due to deterioration of material in the deposit, changes in aeration, water saturation and water movement or land use. Furthermore, bio-apatite, which is depleted in an acidic environment, was present, whilst collagen was unexpectedly poorly preserved [46]. Finally, there was no evidence for tannins in either the brain tissue or the immediate burial environment.

2.6 Modern brain tissue shows short term protein decay

Still, any speculative compound will only have been able to preserve tissue during a limited, unknown time frame after death. Therefore a one-year stability experiment was performed. The summary data is shown in Figure 4. The hypothesised outcome was loss of protein from both the modern control and the ancient brain tissue samples (dark blue shaded areas in Figure 4 A-E). Indeed, for the modern brain there was loss of protein as expected by decay [5]. The standard deviation for separate measurements was most narrow for GFAP (Figure 4 E, triangles). Compared to GFAP the protein concentrations decreased more rapidly for non-phosphorylated NfH (Figure 4 A&C, dots) and phosphorylated NfH (Figure 4 B&D, dots). From these data it can be deduced that in order to preserve GFAP and NfH phosphoforms after death, a speculative preservative compound should have entered the ancient brain within about three months after death.

2.7 Ancient brain tissue shows long-term protein release from aggregates

Unexpectedly, the stability experiment revealed yet another unusual finding for the ancient brain proteins (Figure 4 A-E, dots). There was a consistent increase of the protein concentration for GFAP and NfH phosphoforms for all measurements from the ancient brain (light blue shaded areas in Figure

4 A-E, dots). Notably, this observation would have been missed with the routine time frame used for biomarker stability experiments in the field [1, 45]. The large data scatter during the first three weeks might readily have been dismissed as measurement noise (dots in Figure 4 A-E). The trend for an increase of the concentration of the soluble intermediate filaments only became clear after two months of observation. The steep increase of the curves after one year implies that this trend will continue for a yet unknown amount of time. In contrast to GFAP and NfH phosphoforms there was no systematic trend over time for MBP (see supplementary Figure). Of the several possible interpretations of the data we favour that antibody binding epitopes of intrinsically unstructured regions on intermediate filament iso- and phosphoforms [27] were partly exposed and masked at subsequent intermediate stages of a complex un-/folding process from densely packed protein aggregates [47, 48].

2.8 The stability pattern of IF (GFAP > phospho-NfH > non-phospho-NfH) from control tissue was lost from the ancient brain tissue

Long term biomarker stability was best for GFAP (green shaded area Figure 4 F). This is illustrated by accounting for the different longitudinal profiles of all IF over time in form of a ratio of modern to ancient proteins. For NfH, there was an overlap of the 95% confidence curves of the non-

parametric regression analyses for all phosphoforms (Figure 4 F). The individual regression lines suggested phosphorylated NfH (red and blue lines) to be more stable compared to non-phosphorylated NfH (magenta and gray lines). This interpretation was however only true for the modern brain if the most stable IF, GFAP, was taken as a “house keeping protein” (Figure 4 G). Non-phosphorylated NfH (yellow shaded area) degraded quicker compared to phosphorylated NfH in the modern brain tissue as expected from the literature [43, 44]. This pattern was completely lost for ancient NfH phosphoforms.

2.9 Mass Spectrometry

Samples were analysed by SDS-PAGE followed by in-gel tryptic digestion and LC-MS on a high-resolution Orbitrap mass spectrometer operated in the data dependent mode. Proteins were identified by automatic de novo peptide sequencing and database searching [49]. As extensive protein degradation can be expected, the database search considered also semi-tryptic peptides, i.e., peptides with tryptic cleavage at one end and non-tryptic at the other. N-terminal acetylation is a frequently observed modification in proteomic analysis, as result of post-translational modification but can also be introduced during sample preparation, and was therefore included as variable PTM in the database search. The identification results were validated using the target-decoy approach and only peptide matches above the score threshold corresponding to <1% false-discovery rate (FDR) were used for

protein identification. Furthermore, for a protein to be considered identified required at least one unique peptide, i.e., a peptide not present in any other protein in the database. In total, 881 proteins were identified; 671 in cortex, 759 in white matter, and 531 in both tissues (Supplementary Table 1). To distinguish ancient human proteins in the samples from such contaminants, a blank gel sample were excised from empty lanes and analysed. In total, 855 proteins were identified in the Heslington brain samples and 114 proteins in the gel blank, of which 37 were keratins, abundant in skin and hair. After subtracting proteins present in the blank, 783 proteins remained (Supplementary Table 1). While some of the proteins were keratins that could result from ancient or recent sample contamination, the majority of are proteins expected to be found in brain. GFAP (7 peptides), and NfL were among the identified proteins (3 peptides), and MBP, (3 peptides), confirming the presence of these proteins as detected by ELISA (Figure 5). For GFAP (Figure 5 A), the amino acid sequences of six of the matched tryptic peptides were identical to sequences found in several forms of keratin type II cytoskeletal, rendering their assignment to GFAP ambiguous; however, one peptide (DQLTANSAR, aa 128-136) identified with a score above the chosen 1% FDR threshold was unique to GFAP, thus providing strong evidence for the presence of GFAP in the sample. The annotated fragment ion spectrum for this peptide is shown in Figure 5 C. For NfL there was also a single unique peptide (YEEEVLSR, aa 178-185) identified with a score above the significance threshold.

2.10 Neurological disease analysis

There are a number of well known mutations to brain proteins which can promote protein aggregate formation and which are related to human disease [27, 32, 50, 51]. Some of these change human behaviour profoundly [52, 53]. Other neurological conditions such as Kuru or Creutzfeldt–Jakob disease are transmissible [54–56]. There was however no evidence for pathological human prion proteins with highly sensitive immuno tests [57]. Likewise, DNA extraction only revealed small fragments. Analyses of these DNA fragments with the Illumina kit for formalin-fixed, paraffin-embedded sample DNA did not provide useful sequence data (not shown).

3 Discussion

Taken together the excellent preservation of intracranial soft tissue from the Heslington find [6] enabled us to perform multiple independent molecular analyses to demonstrate exceptional preservation of ancient human brain proteins. Our approach to use a range of complementary analytical techniques [2, 20, 24, 25, 35] not only shows that protein aggregate formation contributed to protein stability, but also that protein epitopes remain highly immunogenic after 2,600 years of exposure to ambient temperature in nature.

The archaeological and macroscopic data reveal the only surviving human tissue from this find to be brain tissue. The macroscopic findings were corroborated on a microscopic level by histology and immuno-histochemistry.

The filamentous structure resembled axons packed with neurofilament proteins [2, 19, 37]. The Heslington brain is not unique and other brains have been found in buried skeletons elsewhere (see references in [6]). But no other brains are known from this period. Only if one extends from natural mummification to *deliberately preserved* bodies, there is one example of preservation of suspected brain tissue (and other soft tissue) dating around the same period. The “Boscastle skull” had recently been dated to 361-112 BC (95.4% confidence interval OxCal v4.17), the Ptolemaic period [58]. In the same paper Smith *et al.* show CT brain images of two Egyptian mummies, the “Hetep-Bastet” and “Lady Hudson” [58]. But these were deliberately preserved brains and not brain tissue surviving because of natural mummification. The preservation of macroscopic structures and imaging studies of the Heslington brain enabled targeted sampling from superficial and deep brain structures for the series of tests.

First, by capitalising on the specificity and sensitivity of the immune response, which has been used successfully to characterize brain proteins [59–61], we show that antibodies raised against ancient brain proteins react specifically with contemporary brain proteins in *in situ* experiments. The binding characteristics are indistinguishable from antiserum raised against contemporary brain tissue [59]. Double labelling demonstrated binding to brain cells of glial lineage, oligodendrocytes (MBP) and astrocytes (GFAP). The signal for neurons (Nf) was weaker than what can be observed using contemporary tissue [60]. The overall extent of epitope preservation over

this amount of time will be of interest to biomedical applications aimed at improving long-term protein storage [1].

Second, highly sensitive immunoassays permitted for quantification of Nf protein isoforms and GFAP. The pattern distribution of these proteins was inverted to what can be seen in a contemporary human control brain. The topographic distribution of Nf isoform concentrations has been related to axonal density in tissue as the main source for Nf proteins [39, 41, 42]. Outwards-in staged inhibition of proteases as the main contributor to cellular autolysis [8, 12] provides one of several possible explanations for this topographic finding. An alternative could be pathological protein aggregate formation during life [26–33]. Presence of pathological prion proteins and their aggregates would have corroborated genetic data on prehistoric kuru-like epidemics [62]. There was no evidence for pathological prion proteins in the ancient brain tissue using state of the art methods [57]. The quality of the DNA was too low to permit for screening of other human diseases of pathological protein aggregation or neurodegeneration [26–33]. These data are consistent with the notion that DNA degrades about 10 times faster than proteins [63, 64].

Third, proteomic analysis by LC-MS of samples digested with trypsin identified over 800 proteins (supplementary data). These data confirmed the imaging and immunological data. Notably there was excellent preservation of GFAP. For the larger Nf LC-MS analysis was less successful. Most likely, this is explained by the challenge to get the large Nf aggregates shown in

the immunoblots to fly in our setup. This is a recognised limitation of the method [65].

In proteomic analysis of ancient samples it is important to consider the risk of adventitious protein identifications stemming from sample contamination that may occur prior to or during excavation, during curation and handling in museums or in the laboratory in conjunction with the analysis [66, 67]. The contamination may come from the laboratory environment or reagents and may occur even if high-purity reagents are used and care is taken to clean all equipment that comes into contact with the samples. Also, proteins from bacteria that colonize the specimen may lead to peptide identifications that are mistakenly matched to human proteins. To counteract the risk of such adventitious protein identifications in our data, a contaminant sequence database was compiled from all proteins identified in blank gel and LC runs, the common Repository of Adventitious Proteins (cRAP; a public database containing known laboratory contaminant proteins; <https://www.thegpm.org/crap/>), and the microbial subset of the UniProt-SwissProt sequence database. The contaminant database was used to filter the identification results within the PEAKS software, such that peptide matches in the contaminant database do not contribute to protein identifications. For GFAP, its high sequence homology to several keratin forms, rendered identification difficult; only a single unique peptide was identified. this is likely to be an issue not only in this, but also in other, future studies investigating intermediate filaments.

Some of the many other proteins recognised are likely to be contaminants from other tissues, notably the many keratins typically found in skin tissue which were absent from the Heslington find. In contrast, the large number of brain derived proteins were also found in analysis of fresh brain tissue. Because of the large amount of preserved sample available this will enable future studies into structure and function of these ancient proteins.

Fourth, the combined interpretation of presence of protein aggregates in the immunoblots and the slow release of GFAP, Nf iso- and phosphoforms from these aggregates in solution over a 12 months period is important. Protein aggregate formation does provide a formidable strategy to minimize surface protein exposure and thereby maximise long-term stability [18, 68, 69]. Yet, amyloid formation is avoided, epitopes are preserved and immunogenicity maintained. This suggests that on a funnel plot energy landscape refolding from an extremely low energy state remains a distinct possibility for biomedical applications [1].

Likewise, protein aggregate formation seems a more plausible explanation for the preservation of beta-keratin in fossil feathers [70] rather than simple mechanical compression. Intermediate filaments share some structural properties with collagens which have been shown to be amongst the most resistant proteins, permitting detection from fossilised bones of 68 million year old *Tyrannosaurus rex*. Collagens were shown to undergo a range of post-translational modifications in mummified tissue [71, 72]. Of these, involvement of lysine is dominant leading to a series of rearrangements, de-

hydration and fragmentation reactions which end up as complex, cross linked structures [65, 71]. Expression of lysine is high in Nf proteins and GFAP [20, 73]. It seems possible that processes similar to what has been observed for collagen, contributed to preservation of the ancient intermediate filament proteins. Whilst the body of emerging evidence in favour of survival of proteins into deep time is seductive, the mechanisms involved are poorly understood [74].

Human species differential expression of collagen composition recently permitted to distinguish Neanderthal from Homo sapiens proteins [75]. Similar has not yet been achieved for the most exciting of all human organs, the brain. Present data opens the possibility for future studies to investigate if between human species there is evidence for preservation or micro-heterogeneity of brain proteins. Such studies may not have to be restricted to preserved brain tissue from human skulls, but venture to investigation of protein sequences bound to mineral surfaces [74].

In this context, a promising feature of Nf proteins is the high binding affinity of serine to silver [76, 77]. Silver containing minerals are not overly abundant which increases the value to humans. But precisely this may enhance the chance to discover silver containing material in human settlements [78]. The mechanisms proposed to enhance ancient protein survival is lowering of their configuration energy [74]. Another advantage of Nf and GFAP is that they belong to the group of intrinsically disorganised proteins [79]. These proteins can adapt many folding states and have a wide spectrum of

binding abilities [80].

In summary, our data provided multiple lines of experimental evidence for long-term preservation of human brain proteins. The data suggest that protein aggregate formation is one strategy for protein preservation.

4 Material and Methods

4.1 Sample acquisition and preparation

Brain samples were processed as described [39]. In brief, five mm³ cubes of brain samples were cut from the surface and depth were submerged in 2 mL of Barbitone EDTA buffer (pH 8.6) and snap-frozen in liquid nitrogen and stored at -80°C. For control brain tissue from a non-neurological control patient was taken.

Samples were defrosted and 20 μ L of a protease inhibitor cocktail (Sigma, P8340) were added (= 1:100). Samples were sonicated on ice. Samples were then diluted 1:1 (= 2 mL added) with Barbitone EDTA buffer containing 16 M urea and 4% CHAPS and mixed at 4°C for 24 hours, centrifuged at 1000 g for 30 minutes at 4°C. The supernatant was stored in aliquots at -80°C.

4.2 Antibody generation

Antibodies were generated using standard procedures [60]. In brief, two different samples of 30 mg brain tissue, one derived from grey matter and

the other from white matter were each dissolved in 200 microliters of 6 M urea, vortexed, sonicated and put on an orbital shaker overnight at 4°C. Each preparation was then mixed with an equal volume of Freund's complete adjuvant and 100 μL of the mix was injected into female Balb/c mice. These mice were three months of age and blood samples were taken by tail bleeding prior to injection. Three weeks later each mouse was injected with 80 μL of the respective mix, and 10 days later about 100 μL of blood was taken from the tail of each mouse. Each mouse was boosted with 80 μL of the respective mix 25 days later, and another blood sample taken 9 days later. The mice were boosted a final time with 80 μL of the respective immunogen 31 days later and a final blood sample taken 10 days later.

4.3 Long term stability experiment

Twenty pair of 250 μL aliquots of the samples from the Heslington brain and modern control brain (1:1 diluted in BarbEDTA buffer containing 0.001% azide and 0.2% bovine serum albumin) were stored light protected at room temperature for up to one year. One pair of aliquots was transferred to -80°C at each of the following time points (1 day, 3 days, 1 week, 2 weeks, 3 weeks, 4 weeks (= 1 month), 2 months and so fort up to 12 month (= one year). Samples were then batch analysed by ELISA in randomised order with the analyst being blinded to randomisation.

4.4 Brain specific protein analysis

Brain specific proteins were quantified using in-house developed ELISAs [60, 81–83]. Total protein was determined using the Bio-Rad Protein assay (Bio-Rad, Hemel Hempstead, UK).

4.5 Gel electrophoresis and immunoblot

Gel electrophoresis and immunoblot were performed as described [39, 57, 60].

4.6 Mass Spectrometry

Protein extracts from cortex and white matter were analyzed by SDS-PAGE followed by LC-MS. 5 μ l 4 x LDS buffer (5 μ l) were added to protein extracts (15 μ l) and the samples were incubated at 70°C for 15 min and analyzed by SDS-PAGE. To preclude contamination of the samples with proteins from the laboratory environment, the gel chamber was cleaned prior to use, and pre-cast gels (NuPAGE, Thermo Fischer) were used that were not exposed to any other samples. Following Coomassie blue staining, the gel lanes were sliced in eight equal-size pieces, which were subjected to reduction and alkylation of cysteine-disulfides and tryptic digestion. The samples were reconstituted in 6 μ l 2% acetonitrile and 0.1% TFA. Aliquots of 5 μ l were loaded on a nanoflow-LC (RSLC nano, Thermo Scientific) equipped with a C18 trap column (PepMap Acclaim 75 μ m *20 mm, Thermo Scientific), and a C18 separation column (PepMap Acclaim 75 μ m * 500 mm, Thermo Scientific), coupled

to a Q-Exactive electrospray ionization mass spectrometer (Thermo Scientific), fitted with a FlexiSpray ion source. Prior to analyzing the samples, several blank LC injections (loading buffer) were performed to ensure the absence of contaminating proteins from previous analyses. The loading buffer was 2% acetonitrile, 0.05% TFA; Buffer A was 0.1% formic acid; and Buffer B was 84% ACN, 0.1% formic acid. The following gradient was used: t=0 min, B=3%; 140 min, B=30%; 160 min, B=45%; 165 min, B=80%. The mass spectrometer was operated in the positive ion mode. Data-dependent acquisition was used, acquiring one full MS scan (R 140k, AGC target 3e6, max IT 250 ms, scan range 400 to 1600 m/z) and up to 10 consecutive HCD MS/MS scans (R=70k, AGC target=1e6, max IT=250 ms, isolation window 1.2 m/z, NCE 32.0, charge exclusion: unassigned, > 6). Samples were analysed in duplicate. Protein identification was performed using the software PEAKS Studio X, , which is based on automatic de novo peptide sequencing. Denovo settings were: Parent Mass Error Tolerance: 15 ppm; Fragment Mass Error Tolerance: 0.05 Da; Enzyme: None; Fixed Modifications: Carbamidomethylation; Variable Modifications: Acetylation (N-term); Max Variable PTM Per Peptide: 1; Report # Peptides: 5. The PEAKS database search settings were: Parent Mass Error Tolerance: 15 ppm; Fragment Mass Error Tolerance: 0.05 Da; Enzyme: Trypsin; Max Missed Cleavages: 3; Non-specific Cleavage: one; Fixed Modification: Carbamidomethylation; Variable Modifications: Acetylation (N-term); Max Variable PTM Per Peptide: 1; Database: UniProt SProt; Taxon: Homo sapiens; Contaminant database: compilation

of all sequences from UniProt Bacteria, cRAP, and proteins identified in blank SDS-PAGE samples and blank LC-MS runs. Validation of peptide identifications was performed using the target-decoy approach. Proteins are reported that had at least one unique peptide hit with a score corresponding to $< 1\%$ FDR. The uniqueness of identified peptides was evaluated using the neXtProt peptide uniqueness checker [84].

4.7 Statistical analysis

Statistical analyses were performed using SAS software (V9.4). Independent variables were compared using the non-parametric two-sample exact Wilcoxon rank-sum test for two variables and a two-way unbalanced ANOVA (general linear model (GLM)) for more than two variables. The linear relationship between continuous variables was evaluated using the Spearman correlation coefficient. Non-parametric regression analyses were performed using LOESS and 95% confidence curves were calculated. The level of significance for the multiple correlations was corrected using the Bonferroni method. Two-tailed tests were used throughout and p values of < 0.05 were accepted as significant.

4.8 Exclusion of sample contamination

Methods for exclusion of sample contamination were applied on several levels. First, samples were independently analysed in three laboratories: London,

Gothenburg and Gainsville. Next, a range of complementary methods were used in these laboratories which taken together provide several independent lines of evidence for preservation of brain proteins. The London and Gothenburg laboratories are both accredited to ISO 15189 quality standard.

Most importantly, we excluded all peptides and proteins reported in the literature as problematic regarding sample contamination [66, 67]. Finally, we have made our raw data available for independent analyses through the PRIDE repository (<https://www.ebi.ac.uk/pride/archive/>). Data are available via ProteomeXchange with identifier PXD014178.

For the proteomic analyses there are additional sources of protein contamination to consider. One being carry-over from previous samples analysed using the same laboratory equipment. To minimise this risk we carefully cleaned the gel electrophoresis equipment prior to analysis. In addition we have used new HPLC columns for these experiments. This eliminates the possibility for carry over from columns which have previously exposed to unknown proteins. Finally, prior to analysing the brain samples by LC-MS, blank samples were analysed, including both gel blanks and LC blanks, to ensure absence of contaminating proteins.

Author's contributions A.P. had the idea to the study, designed and performed experiments and wrote the manuscript. C.H.L., G.S. J.G. and M.G. contributed to the laboratory work. G.S. produced the antibodies against the ancient brain proteins. All co-authors revised the manuscript.

Data Accessibility Data will be shared upon reasonable request and are also available through the PRIDE repository (<https://www.ebi.ac.uk/pride/archive/>), identifier PXD014178.

Ethical statement Ethical approval for this study was given (centre number 875KLH, study number 03/N101, UK).

Competing interests G.S. is founder of EnCor Biotechnology Inc. in Gainesville, USA. H.Z. is a co-founder of Brain Biomarker Solutions in Gothenburg AB, a GU Ventures-based platform company at the University of Gothenburg. Professor Zetterberg has served on advisory boards for Roche Diagnostics, Eli Lilly, and Pharmasum Therapeutics.

Funding The Heslington brain project which was co-funded by the University of York and English Heritage. Sonia O'Connor is the principal investigator of the project for the York Archaeological Trust.

Acknowledgements The authors thank C. Yang, S. Joiner and J Wadsworth for technical assistance.

References

- [1] DK Karig, S Bessling, P Thielen, S Zhang, and J Wolfe. “Preservation of protein expression systems at elevated temperatures for portable therapeutic production”. *Journal of The Royal Society Interface* 14 (2017), p. 20161039. DOI: 10.1098/rsif.2016.1039.
- [2] M Bacioglu, LF Maia, O Preische, et al. “Neurofilament Light Chain in Blood and CSF as Marker of Disease Progression in Mouse Models and in Neurodegenerative Diseases.” *Neuron* 91 (2 2016), pp. 494–496. ISSN: 1097-4199. DOI: 10.1016/j.neuron.2016.07.007.
- [3] JA Moreno, M Halliday, C Molloy, et al. “Oral Treatment Targeting the Unfolded Protein Response Prevents Neurodegeneration and Clinical Disease in Prion-Infected Mice”. *Sci Transl Med* 5 (2013), 206ra138–206ra138. DOI: 10.1126/scitranslmed.3006767.
- [4] TJ Ahern and AM Klibanov. “The mechanisms of irreversible enzyme inactivation at 100C.” *Science* 228 (1985), pp. 1280–1284. DOI: 10.1126/science.4001942.
- [5] T Lindahl. “Instability and decay of the primary structure of DNA”. *Nature* 362 (1993), pp. 709–715. ISSN: 0028-0836. DOI: 10.1038/362709a0.
- [6] S O’Connor, E Ali, S Al-Sabah, et al. “Exceptional preservation of a prehistoric human brain from Heslington, Yorkshire, UK”. *Journal of Archaeological Science* 38 (2011), pp. 1641–1654. DOI: 10.1016/j.jas.2011.02.030.

- [7] J Travis. “Archaeology. Archaeologists see big promise in going molecular.” *Science* 330 (2010), pp. 28–29. DOI: 10.1126/science.330.6000.28.
- [8] RJA Goodwin, JC Dungworth, SR Cobb, and AR Pitt. “Time-dependent evolution of tissue markers by MALDI-MS imaging.” *Proteomics* 8 (2008), pp. 3801–3808. DOI: 10.1002/pmic.200800201.
- [9] A Vass. “Beyond the grave - understanding human decomposition”. *Microbiology Today* 28 (2001), pp. 190–192. ISSN: 1464-0570.
- [10] J Travis. “Third International Symposium on Biomolecular Archaeology. Old bones reveal new signs of scurvy.” *Science* 322 (2008), pp. 368–369. DOI: 10.1126/science.322.5900.368b.
- [11] GWH Schepers. “The Fossil Brain”. *The South African Archaeological Bulletin* 4 (1949), pp. 71–82. DOI: 10.2307/3886422.
- [12] N Vanlangenakker, T Berghe, D Krysko, N Festjens, and P Vandenaabeele. “Molecular Mechanisms and Pathophysiology of Necrotic Cell Death”. *Curr Mol Med* 8 (2008), pp. 207–220. DOI: 10.2174/156652408784221306.
- [13] RBH Gradwohl, FE Camps, AE Robinson, and BGB Lucas. *Gradwohl’s Legal Medicine*. 3rd. Wright, Bristol, UK, 1976. ISBN: 0723603103.
- [14] MA DePristo, DM Weinreich, and DL Hartl. “Missense meanderings in sequence space: a biophysical view of protein evolution”. *Nature Reviews Genetics* 6 (2005), pp. 678–687. DOI: 10.1038/nrg1672.

- [15] T Sikosek and HS Chan. “Biophysics of protein evolution and evolutionary protein biophysics”. *Journal of The Royal Society Interface* 11 (2014), pp. 20140419–20140419. DOI: 10.1098/rsif.2014.0419.
- [16] P Csermely, R Palotai, and R Nussinov. “Induced fit, conformational selection and independent dynamic segments: an extended view of binding events”. *Trends in biochemical sciences* 35 (2010), pp. 539–546. DOI: 10.1016/j.tibs.2010.04.009.
- [17] JD Bloom, JJ Silberg, CO Wilke, DA Drummond, C Adami, and FH Arnold. “Thermodynamic prediction of protein neutrality”. *Proceedings of the National Academy of Sciences* 102 (2005), pp. 606–611. DOI: 10.1073/pnas.0406744102.
- [18] RAF Redondo, HP de Vladar, T Włodarski, and JP Bollback. “Evolutionary interplay between structure, energy and epistasis in the coat protein of the X174 phage family”. *Journal of The Royal Society Interface* 14 (2017), p. 20160139. DOI: 10.1098/rsif.2016.0139.
- [19] E Fuchs. “A structural scaffolding of intermediate filaments in health and disease”. *Science* 279 (1998), pp. 514–519. DOI: 10.1126/science.279.5350.514.
- [20] A Petzold. “Neurofilament phosphoforms: Surrogate markers for axonal injury, degeneration and loss”. *J Neurol Sci* 233 (2005), pp. 183–198. DOI: 10.1016/j.jns.2005.03.015. URL: <https://discovery.ucl.ac.uk/id/eprint/18928/>.

- [21] M Khalil, CE Teunissen, M Otto, et al. “Neurofilaments as biomarkers in neurological disorders.” *Nature Reviews Neurology* 14 (2018), pp. 577–589. ISSN: 1759-4766. DOI: 10.1038/s41582-018-0058-z. URL: <https://discovery.ucl.ac.uk/id/eprint/10057189/>.
- [22] J Lu, JM Frerich, LC Turtzo, et al. “Histone deacetylase inhibitors are neuroprotective and preserve NGF-mediated cell survival following traumatic brain injury”. *Proc Natl Acad Sci U S A* 110 (2013), pp. 10747–10752. DOI: 10.1073/pnas.1308950110.
- [23] DI Friedman, MP McDermott, K Kiebertz, et al. “The idiopathic intracranial hypertension treatment trial: design considerations and methods.” *J Neuroophthalmol* 34 (2014), pp. 107–117. DOI: 10.1097/WNO.0000000000000114.
- [24] M Comabella and X Montalban. “Body fluid biomarkers in multiple sclerosis.” *Lancet Neurol* 13 (2014), pp. 113–126. DOI: 10.1016/S1474-4422(13)70233-3.
- [25] B Olsson, R Lautner, U Andreasson, et al. “CSF and blood biomarkers for the diagnosis of Alzheimer’s disease: a systematic review and meta-analysis”. *The Lancet Neurology* 15 (2016), pp. 673–684. DOI: 10.1016/S1474-4422(16)00070-3.
- [26] DC David, N Ollikainen, JC Trinidad, MP Cary, AL Burlingame, and C Kenyon. “Widespread Protein Aggregation as an Inherent Part of

- Aging in *C. elegans*.” *PLoS Biol* 8 (2010), e1000450. DOI: 10.1371/journal.pbio.1000450.
- [27] VM Lee, L Otvos, MJ Carden, M Hollosi, B Dietzschold, and RA Lazarini. “Identification of the major multiphosphorylation site in mammalian neurofilaments.” *Proceedings National Academy Sciences United States America* 85 (1988), pp. 1998–2002. DOI: 10.1073/pnas.85.6.1998.
- [28] VM Lee, L Otvos, ML Schmidt, and JQ Trojanowski. “Alzheimer disease tangles share immunological similarities with multiphosphorylation repeats in the two large neurofilament proteins.” *Proceedings National Academy Sciences United States America* 85 (1988), pp. 7384–7388. DOI: 10.1073/pnas.85.19.7384.
- [29] A Dunker, J Lawson, CJ Brown, et al. “Intrinsically disordered protein”. *Journal of Molecular Graphics and Modelling* 19 (2001), pp. 26–59. DOI: 10.1016/s1093-3263(00)00138-8.
- [30] MM Babu, RW Kriwacki, and RV Pappu. “Versatility from Protein Disorder”. *Science* 337 (2012), pp. 1460–1461. DOI: 10.1126/science.1228775.
- [31] CH Lu, B Kalmar, A Malaspina, L Greensmith, and A Petzold. “A method to solubilise protein aggregates for immunoassay quantification which overcomes the neurofilament hook effect”. *J Neurosci Methods*

- 195 (2011), pp. 143–150. DOI: 10.1016/j.jneumeth.2010.11.026.
URL: <https://discovery.ucl.ac.uk/id/eprint/678078>.
- [32] M Jucker and LC Walker. “Self-propagation of pathogenic protein aggregates in neurodegenerative diseases.” *Nature* 501 (2013), pp. 45–51. DOI: 10.1038/nature12481.
- [33] A Petzold, D Tozer, and K Schmierer. “Axonal damage in the making: Neurofilament phosphorylation, proton mobility and magnetisation transfer in multiple sclerosis normal appearing white matter”. *Exp Neurol* 232 (2011), pp. 234–239. DOI: 10.1016/j.expneurol.2011.09.011. URL: <https://discovery.ucl.ac.uk/id/eprint/1326582>.
- [34] EM Meiering. “The Threat of Instability: Neurodegeneration Predicted by Protein Destabilization and Aggregation Propensity”. *PLoS Biol* 6 (2008), e193. DOI: 10.1371/journal.pbio.0060193.
- [35] N Theilacker, EE Roller, KD Barbee, M Franzreb, and X Huang. “Multiplexed protein analysis using encoded antibody-conjugated microbeads”. *Journal of The Royal Society Interface* 8 (2011), pp. 1104–1113. DOI: 10.1098/rsif.2010.0594.
- [36] A Keller, A Graefen, M Ball, et al. “New insights into the Tyrolean Ice-mans origin and phenotype as inferred by whole-genome sequencing”. *Nat Commun* 3 (2012), p. 698. DOI: 10.1038/ncomms1701.

- [37] G Shaw and K Weber. “Differential expression of neurofilament triplet proteins in brain development”. *Nature* 298 (5871 1982), pp. 277–279. ISSN: 0028-0836. DOI: 10.1038/298277a0.
- [38] JF Collard, F Côté, and JP Julien. “Defective axonal transport in a transgenic mouse model of amyotrophic lateral sclerosis”. *Nature* 375 (1995), pp. 61–64. DOI: 10.1038/375061a0.
- [39] A Petzold, D Gveric, M Groves, et al. “Phosphorylation and compactness of neurofilaments in multiple sclerosis: Indicators of axonal pathology”. *Exp Neurol* 213 (2008), pp. 326–335. DOI: 10.1016/j.expneurol.2008.06.008. URL: <https://rps.ucl.ac.uk/repository.html?pub=96188>.
- [40] RA Nixon, JF Clarke, KB Logvinenko, MK Tan, M Hault, and F Grynspan. “Aluminum inhibits calpain-mediated proteolysis and induces human neurofilament proteins to form protease-resistant high molecular weight complexes.” *Journal of neurochemistry* 55 (6 1990), pp. 1950–1959. ISSN: 0022-3042. DOI: 10.1111/j.1471-4159.1990.tb05781.x.
- [41] KJ Anderson, SW Scheff, KM Miller, KN Roberts, LK Gilmer, C Yang, and G Shaw. “The Phosphorylated Axonal Form of the Neurofilament Subunit NF-H (pNF-H) as a Blood Biomarker of Traumatic Brain Injury”. *J Neurotrauma* 25 (2008), pp. 1079–1085. DOI: 10.1089/neu.2007.0488.

- [42] A Petzold, M Eikelenboom, D Gveric, et al. “Markers for different glial cell responses in multiple sclerosis: clinical and pathological correlations”. *Brain* 125 (2002), pp. 1462–1473. DOI: 10.1093/brain/awf165. URL: <https://rps.ucl.ac.uk/viewobject.html?cid=1&id=26845>.
- [43] M Goldstein, N Sternberger, and L Sternberger. “Phosphorylation protects neurofilaments against proteolysis”. *J Neuroimmunol* 14 (1987), pp. 149–160. DOI: 10.1016/0165-5728(87)90049-X.
- [44] HC Pant. “Dephosphorylation of neurofilament proteins enhances their susceptibility to degradation by calpain”. *Biochem. J.* 256 (1988), pp. 665–608. DOI: 10.1042/bj2560665.
- [45] MJ Koel-Simmelink, CE Teunissen, P Behradkia, MA Blankenstein, and A Petzold. “The neurofilament light chain is not stable in vitro”. *Ann Neurol* 69 (2011), pp. 1065–1066. DOI: 10.1002/ana.22438.
- [46] RC Connolly. “Lindow Man: Britains Prehistoric Bog Body”. *Anthropology Today* 1 (1985), pp. 15–17. DOI: 10.2307/3032823.
- [47] R Beck, J Deek, JB Jones, and CR Safinya. “Gel-expanded to gel-condensed transition in neurofilament networks revealed by direct force measurements.” *Nat Mater* 9 (2010), pp. 40–46. DOI: 10.1038/nmat2566.
- [48] J Deek, PJ Chung, J Kayser, AR Bausch, and CR Safinya. “Neurofilament sidearms modulate parallel and crossed-filament orientations inducing nematic to isotropic and re-entrant birefringent hydrogels.” *Nat Commun* 4 (2013), p. 2224. DOI: 10.1038/ncomms3224.

- [49] B Ma, K Zhang, C Hendrie, C Liang, M Li, A Doherty-Kirby, and G Lajoie. “PEAKS: powerful software for peptide de novo sequencing by tandem mass spectrometry.” *Rapid communications in mass spectrometry : RCM* 17 (20 2003), pp. 2337–2342. ISSN: 0951-4198. DOI: 10.1002/rcm.1196.
- [50] J Hardy and G Higgins. “Alzheimer’s disease: the amyloid cascade hypothesis”. *Science* 256 (1992), pp. 184–185. DOI: 10.1126/science.1566067.
- [51] RH Brown and A Al-Chalabi. “Amyotrophic Lateral Sclerosis”. *New England Journal of Medicine* 377 (2017). Ed. by DL Longo, pp. 162–172. DOI: 10.1056/nejmra1603471.
- [52] P Brundin, R Melki, and R Kopito. “Prion-like transmission of protein aggregates in neurodegenerative diseases”. *Nature reviews. Molecular cell biology* 11 (2010), pp. 301–307. DOI: 10.1038/nrm2873.
- [53] BS Shastry. “Neurodegenerative disorders of protein aggregation”. *Neurochemistry international* 43 (2003), pp. 1–7. DOI: 10.1016/s0197-0186(02)00196-1.
- [54] J Sotelo, C Gibbs, and D Gajdusek. “Autoantibodies against axonal neurofilaments in patients with Kuru and Creutzfeldt-Jakob disease”. *Science* 210 (1980), pp. 190–193. DOI: 10.1126/science.6997994.

- [55] A Thompson, A MacKay, P Rudge, et al. “Behavioral and Psychiatric Symptoms in Prion Disease”. *American Journal of Psychiatry* 171 (2014), pp. 265–274. DOI: 10.1176/appi.ajp.2013.12111460.
- [56] JDF Wadsworth, S Joiner, JM Linehan, et al. “Kuru prions and sporadic Creutzfeldt–Jakob disease prions have equivalent transmission properties in transgenic and wild-type mice”. *Proceedings of the National Academy of Sciences* 105 (2008), pp. 3885–3890. DOI: 10.1073/pnas.0800190105.
- [57] JDF Wadsworth, G Adamson, S Joiner, et al. “Methods for Molecular Diagnosis of Human Prion Disease”. *Prions*. Springer New York, 2017, pp. 311–346. DOI: 10.1007/978-1-4939-7244-9_22.
- [58] MJ Smith, P Kneller, D Elliott, C Young, H Manley, and D Osselton. “Multidisciplinary analysis of a mummified cranium claimed to be that of a medieval execution victim”. *Archaeological and Anthropological Sciences* 4 (2012), pp. 75–89. DOI: 10.1007/s12520-011-0084-x.
- [59] LA Sternberger and NH Sternberger. “Monoclonal antibodies distinguish phosphorylated and nonphosphorylated forms of neurofilaments in situ.” *Proc Natl Acad Sci USA* 80 (1983), pp. 6126–6130. DOI: 10.1073/pnas.80.19.6126.
- [60] G Shaw, C Yang, R Ellis, et al. “Hyperphosphorylated neurofilament NF-H is a serum biomarker of axonal injury”. *Biochem Biophys Res*

- Comm* 336 (2005), pp. 1268–1277. DOI: 10.1016/j.bbrc.2005.08.252.
- [61] E Debus, K Weber, and M Osborn. “Monoclonal antibodies specific for glial fibrillary acidic (GFA) protein and for each of the neurofilament triplet polypeptides”. *Differentiation* 25 (1984), pp. 193–203. DOI: 10.1111/j.1432-0436.1984.tb01355.x.
- [62] S Mead, MP Stumpf, J Whitfield, et al. “Balancing Selection at the Prion Protein Gene Consistent with Prehistoric Kurulike Epidemics”. *Science* 300 (2003), pp. 640–643. DOI: 10.1126/science.1083320.
- [63] E Cappellini, MJ Collins, and MTP Gilbert. “Unlocking Ancient Protein Palimpsests”. *Science* 343 (2014), pp. 1320–1322. DOI: 10.1126/science.1249274.
- [64] RF Service. “Protein power”. *Science (New York, N.Y.)* 349 (6246 2015), pp. 372–373. ISSN: 1095-9203. DOI: 10.1126/science.349.6246.372.
- [65] S Dallongeville, N Garnier, C Rolando, and C Tokarski. “Proteins in Art, Archaeology, and Paleontology: From Detection to Identification.” *Chemical reviews* 116 (1 2016), pp. 2–79. ISSN: 1520-6890. DOI: 10.1021/acs.chemrev.5b00037.
- [66] J Hendy, F Welker, B Demarchi, C Speller, C Warinner, and MJ Collins. “A guide to ancient protein studies.” *Nature ecology & evolu-*

- tion* 2 (5 2018), pp. 791–799. ISSN: 2397-334X. DOI: 10.1038/s41559-018-0510-x.
- [67] M Buckley, S Warwood, B van Dongen, AC Kitchener, and PL Manning. “A fossil protein chimera difficulties in discriminating dinosaur peptide sequences from modern cross-contamination”. *Proceedings of the Royal Society B: Biological Sciences* 284 (1855 2017), p. 20170544. ISSN: 1471-2954. DOI: 10.1098/rspb.2017.0544.
- [68] M Calamai, C Canale, A Relini, M Stefani, F Chiti, and CM Dobson. “Reversal of protein aggregation provides evidence for multiple aggregated States.” *J Mol Biol* 346 (2005), pp. 603–616. DOI: 10.1016/j.jmb.2004.11.067.
- [69] P Hortschansky, T Christopeit, V Schroeckh, and M Fändrich. “Thermodynamic analysis of the aggregation propensity of oxidized Alzheimer’s -amyloid variants”. *Protein Sci* 14 (2005), pp. 2915–2918. DOI: 10.1110/ps.051585905.
- [70] Y Pan, W Zheng, AE Moyer, et al. “Molecular evidence of keratin and melanosomes in feathers of the Early Cretaceous bird *Eoconfuciusornis*”. *Proceedings of the National Academy of Sciences* 113 (2016), E7900–E7907. DOI: 10.1073/pnas.1617168113.
- [71] I Mikšik, P Sedláková, S Pataridis, F Bortolotti, and R Gottardo. “Proteins and their modifications in a medieval mummy”. *Protein Science* 25 (2016), pp. 2037–2044. DOI: 10.1002/pro.3024.

- [72] J Jones, M Mirzaei, P Ravishankar, et al. “Identification of proteins from 4200-year-old skin and muscle tissue biopsies from ancient Egyptian mummies of the first intermediate period shows evidence of acute inflammation and severe immune response”. *Philosophical Transactions of the Royal Society A: Mathematical, Physical and Engineering Sciences* 374 (2016), p. 20150373. ISSN: 1364-503X. DOI: 10.1098/rsta.2015.0373.
- [73] A Petzold. “Glial fibrillary acidic protein is a body fluid biomarker for glial pathology in human disease”. *Brain research* 1600 (2015), pp. 17–31. DOI: 10.1016/j.brainres.2014.12.027.
- [74] B Demarchi, S Hall, T Roncal-Herrero, et al. “Protein sequences bound to mineral surfaces persist into deep time”. *eLife* 5 (2016). ISSN: 2050-084X. DOI: 10.7554/elife.17092.
- [75] F Welker, M Hajdinjak, S Talamo, et al. “Palaeoproteomic evidence identifies archaic hominins associated with the Châtelperronian at the Grotte du Renne.” *Proceedings of the National Academy of Sciences of the United States of America* 113 (40 2016), pp. 11162–11167. ISSN: 1091-6490. DOI: 10.1073/pnas.1605834113.
- [76] D Bodian. “A new method for staining nerve fibers and nerve endings in mounted paraffin sections”. *The Anatomical Record* 65 (1936), pp. 89–97. DOI: 10.1002/ar.1090650110.

- [77] P Gambetti, LA Gambetti, and S Papasozomenos. “Bodians silver method stains neurofilament polypeptides”. *Science* 213 (1981), pp. 1521–1522. DOI: 10.1126/science.6169146.
- [78] AM Thibodeau, DJ Killick, J Ruiz, JT Chesley, K Deagan, JM Cruxent, and W Lyman. “The strange case of the earliest silver extraction by European colonists in the New World.” *Proceedings of the National Academy of Sciences of the United States of America* 104 (9 2007), pp. 3663–3666. ISSN: 0027-8424. DOI: 10.1073/pnas.0607297104.
- [79] HJ Dyson and PE Wright. “Intrinsically unstructured proteins and their functions.” *Nat Rev Mol Cell Biol* 6 (2005), pp. 197–208. DOI: 10.1038/nrm1589.
- [80] VN Uversky. “Dancing protein clouds: the strange biology and chaotic physics of intrinsically disordered proteins”. *Journal of Biological Chemistry* 291 (2016), pp. 6681–6688. DOI: 10.1074/jbc.r115.685859.
- [81] A Petzold, G Keir, A Green, G Giovannoni, and E Thompson. “A specific ELISA for measuring neurofilament heavy chain phosphoforms”. *J Immunol Methods* 278 (2003), pp. 179–190. DOI: 10.1016/s0022-1759(03)00189-3.
- [82] A Petzold, A Altintas, L Andreoni, et al. “Neurofilament ELISA validation”. *Journal of Immunological Methods* 352 (1-2 2010), pp. 23–31. ISSN: 1872-7905. DOI: 10.1016/j.jim.2009.09.014. URL: <https://discovery.ucl.ac.uk/id/eprint/95615/>.

- [83] A Petzold, G Keir, AJE Green, G Giovannoni, and EJ Thompson. “An ELISA for glial fibrillary acidic protein.” *J Immunol Methods* 287 (2004), pp. 169–177. DOI: 10.1016/j.jim.2004.01.015.
- [84] M Schaeffer, A Gateau, D Teixeira, PA Michel, M Zahn-Zabal, and L Lane. “The neXtProt peptide uniqueness checker: a tool for the proteomics community.” *Bioinformatics (Oxford, England)* 33 (2017), pp. 3471–3472. ISSN: 1367-4811. DOI: 10.1093/bioinformatics/btx318.

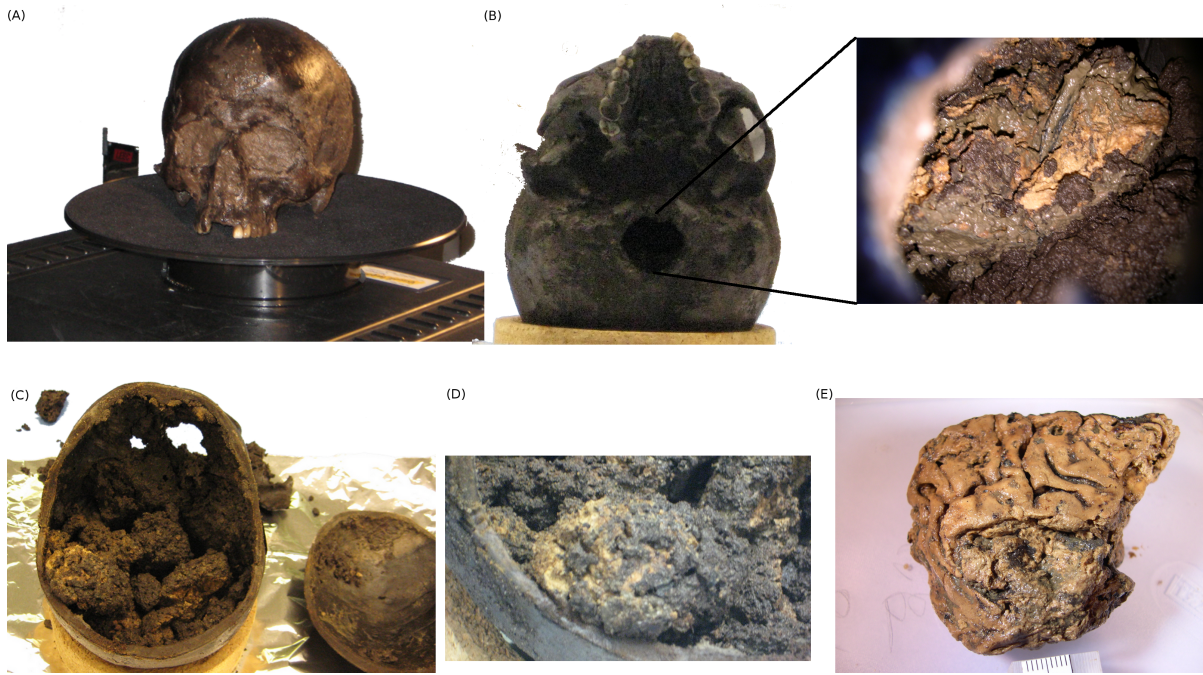


Figure 1: *The Heslington brain. (A) All orifices of the dark skull were tightly covered with mud; (B) shows the skull base with the foramen magnum. Illumination of the inner part of the skull as seen through the foramen magnum is shown in the inlay; (C) after opening the skull the sediment covered structure remained intact; (D) these structures resemble a shrunken brain covered with muddy sediment; (E) careful removal of the sediment uncovers a surface resembling the gyri of a human brain.*

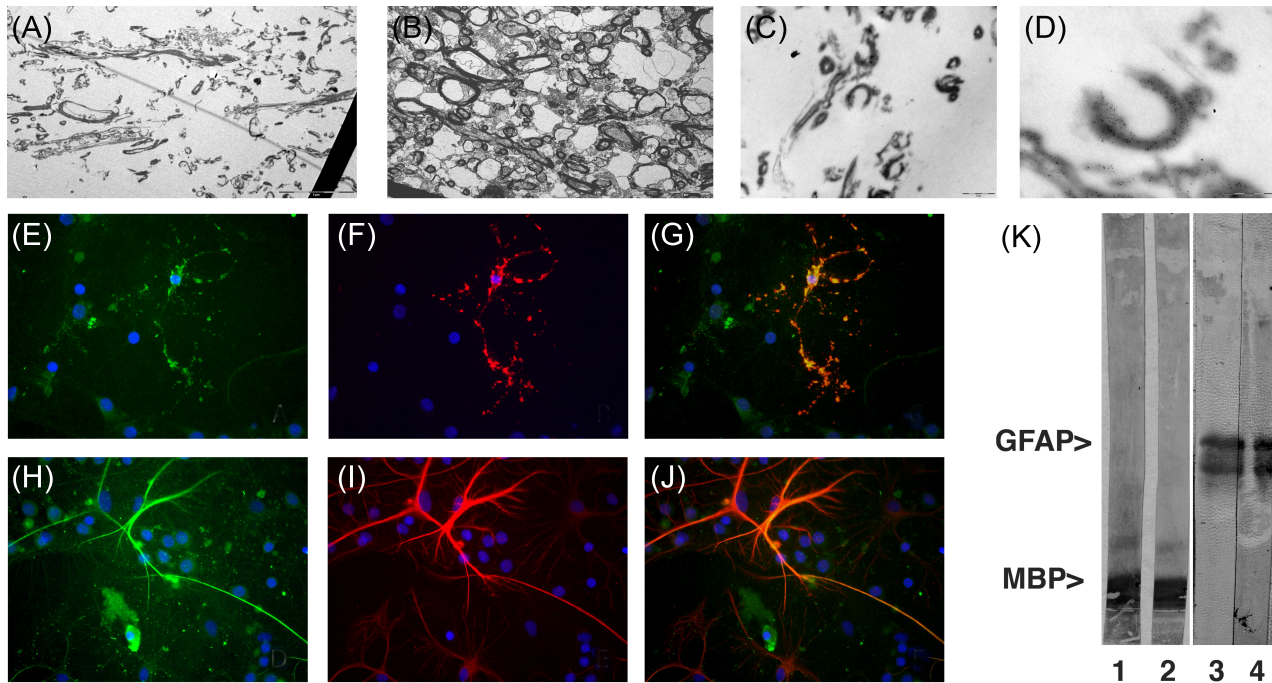


Figure 2: *Electron-microscopy shows 5–10 μm long and 0.2–0.6 μm thick filamentous electrodense structures in (A) the Heslington brain which are comparable to the slightly longer and more distinct structures seen in (B) a recent control brain. The dark electrodense outer structure seen in the control brain resembles myelin and the more filamentous cytoskeletal structures resemble neurofilaments. (C) Immunoelectron microscopy demonstrates that these structures consist of densely packed neurofilament proteins which are (D) strictly localised to the electrodense axon like structures.*

The Heslington brain tissue is still able to stimulate a very robust immune response in mice with high affinity antibodies against GFAP, Nf and MBP. Staining of E21 rat cortical neuron cultures stained with mouse serum (E) shows cells resembling oligodendroglia. Double label with MBP polyclonal antibody (F) shows a similar staining pattern in these cells (F), and superimposition of the two images shows excellent overlap between mouse serum and MBP antibody in cells with an oligodendrocyte morphology (G). Similarly, mouse serum staining of these cultures shows some staining of cells with the morphology of astrocytes and microglia (H). The astrocytic cells also stained with GFAP antibody (I), with convincing overlap (J). To verify the specificity of the immune response, mouse serum (K, lane 1) and MBP antibody (lane 2) were tested on western blots of pure MBP. Mouse serum was also tested on pure GFAP (lane 3) and compared to GFAP antibody (lane 4). The mouse serum clearly recognizes both pure MBP and GFAP.

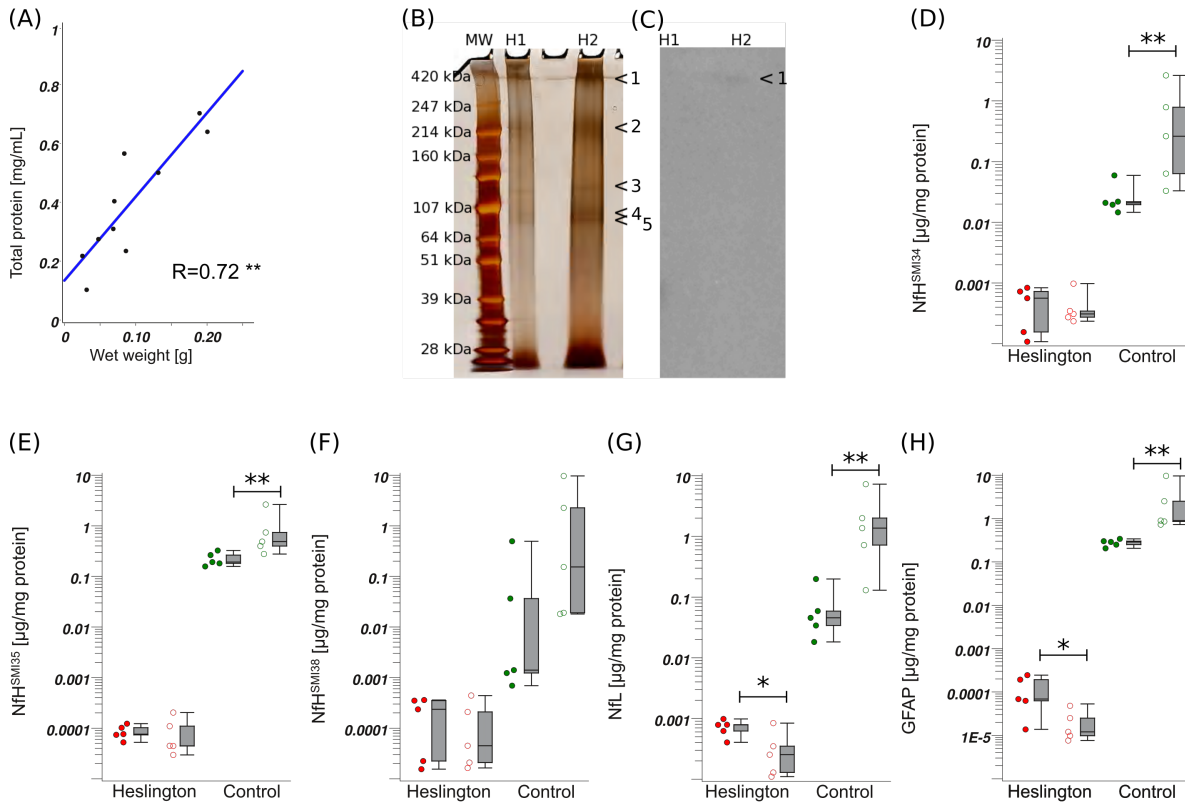


Figure 3: **(A)** The total protein correlated with the wet weight of the Heslington brain samples. **(B)** Gel electrophoresis (3-8% TA), bands 1-4 were used for Silver stain. The Gel was cut through band 5. Bands 1-4 were further used for **(C)** Western blot (SMI 34). MW = molecular weight markers, H1 = Heslington brain, gel loaded with 0.05 $\mu\text{g}/\text{ml}$ (H1) and 0.2 $\mu\text{g}/\text{ml}$ (H2) total protein. (White matter sample #5).

Grey matter (dots) and white matter (open circles) samples from the Heslington brain (red) compared to a control brain (green) showing **(D)** hyperphosphorylated NfH (SMI34), **(E)** phosphorylated NfH (SMI35), **(F)** non-phosphorylated NfH (SMI38), **(G)** NfL and **(H)** GFAP. Typically, intermediate filaments (Nf, GFAP) are higher in the control white matter (D, E, G, H) compared to grey matter ($p < 0.01 = **$). For the Heslington brain, however the inverse is observed for NfL and GFAP (G, H, $p < 0.05 = *$).

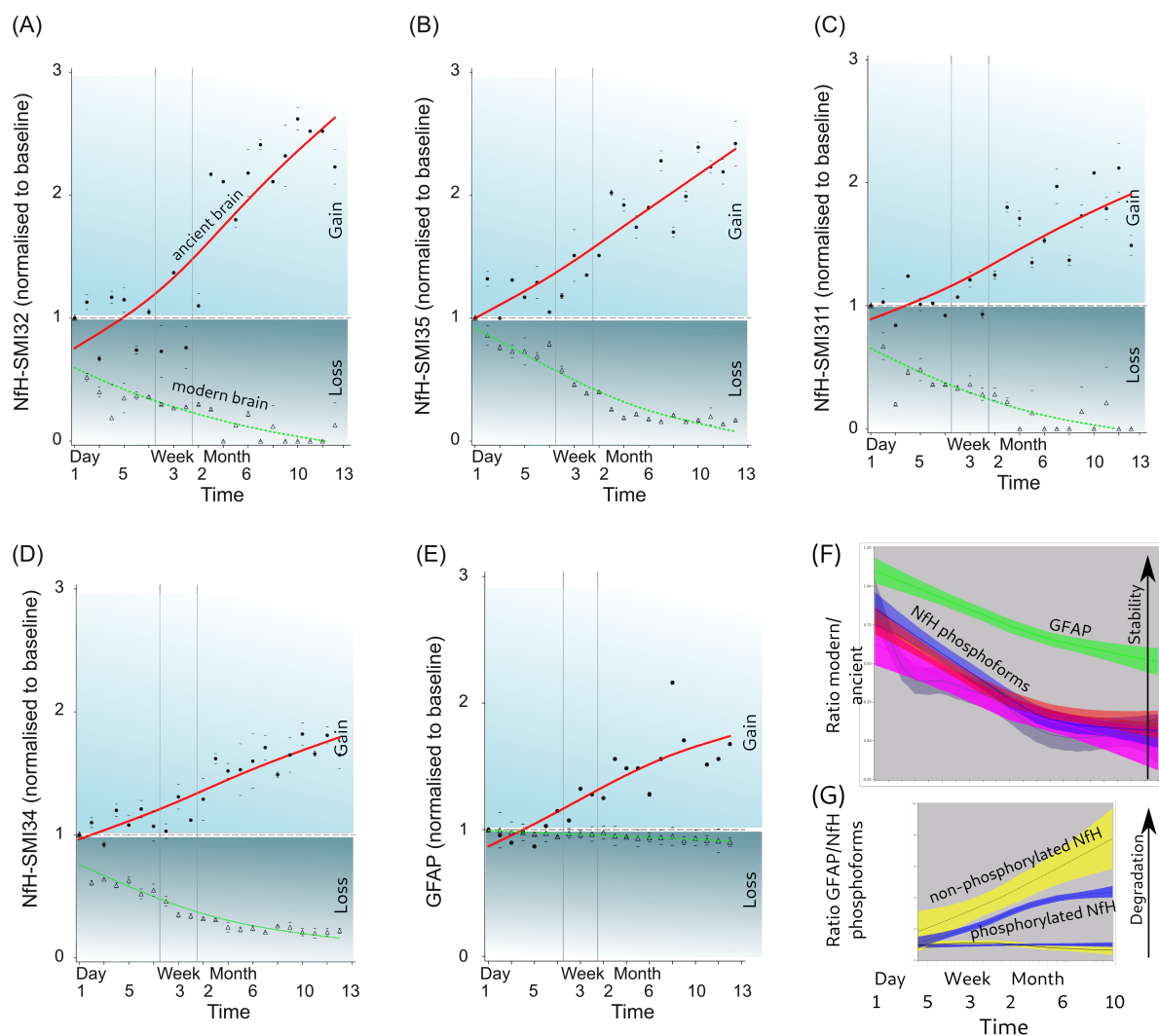


Figure 4: Stability of intermediate filaments (NfH phosphoforms, GFAP) from ancient (closed red line, dots) and modern brain tissue (dashed green line, triangles). Loss of protein is shown in the dark blue shaded area and gain of protein in the light blue shaded area above the horizontal reference line indicating the normalised (100%) baseline values. Data are shown for **(A)-(D)** neurofilament phosphoforms and **(E)** GFAP as mean \pm standard deviation. There is a gain of all intermediate filaments from the ancient brain tissue, whilst they decompose from the modern brain tissue. The vertical reference lines indicate where the time-scale of the x-axis expands from days to weeks to months. **(F)** The most stable intermediate filament is GFAP (green), also after accounting for the difference in stability profiles between ancient and modern brain tissue (ratio), followed by NfH-SMI34 (red), NfH-SMI35 (blue), NfH-SMI32 (magenta) and NfH-SMI311 (grey). **(G)** Taking the stable GFAP as “house keeping” protein reveals that the relative larger susceptibility to degradation of non-phosphorylated NfH (SMI32, yellow) compared to hyper-phosphorylated NfH (SMI34, blue) in modern brain tissue (dashed lines) has been lost from the ancient brain tissue (closed lines).

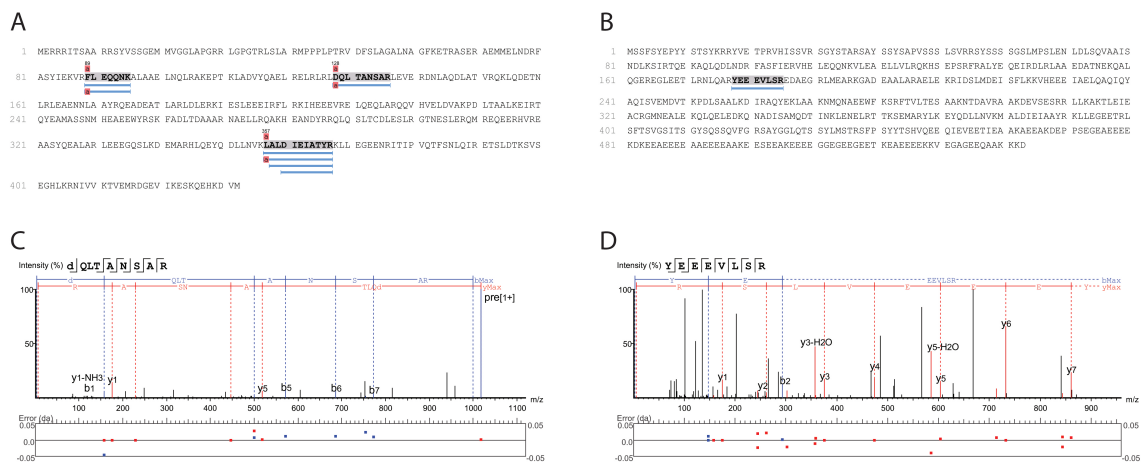


Figure 5: Sequence coverage for (A) GFAP and (B) NfL by mass spectrometry. The blue lines indicate the amino acid sequence of the identified tryptic peptides. “O” indicates oxidized methionine. The annotated fragment ion spectra of the tryptic peptides identified are shown for (C) GFAP and (D) NfL.